Dynamical magnetic susceptibility in antiferromagnet $UPtGa_5$ determined by NMR: Comparison with isostructural superconducting $CeMIn_5$ systems

S. Kambe,[1] T. Hattori,[1] H. Sakai,[1] Y. Tokunaga,[1] and R. E. Walstedt[2]
[1]*Advanced Science Research Center, Japan Atomic Energy Agency, Tokai-mura, Ibaraki 319-1195, Japan*
[2]*Physics Department, The University of Michigan, Ann Arbor, Michigan 48109, USA*
(Received 23 March 2016; revised manuscript received 1 May 2016; published 31 May 2016)

We report, as an example, a complete analysis of nuclear spin-lattice relaxation time (T_1) data for the strongly correlated antiferromagnet $UPtGa_5$, which has a typical $HoCoGa_5$ (115) structure. Using a high-quality single-crystal sample, the T dependence of T_1 at ^{195}Pt and at two crystallographically inequivalent ^{69}Ga sites has been measured for $H \parallel a$ and c axes. Using previously obtained hyperfine coupling tensors from static Knight shift results, the anisotropic spin fluctuation energy and $\vec{q}$ dependence of the dynamic susceptibility have been determined completely, forming a clear contrast to the cases of superconducting $CeRhIn_5$, $CeCoIn_5$, and $CeIrIn_5$, which are considered to be very near to a quantum critical point. We also note that a similar hyperfine coupling scheme to that of $CeRhIn_5$ has been found for $UPtGa_5$.

DOI: 10.1103/PhysRevB.93.205155

I. INTRODUCTION

In the last decade, Ce and actinide-based 115 compounds have been studied intensively, since many interesting electronic behaviors have been observed in these systems [1], e.g., unconventional superconductivity near a quantum critical point [2–4], high-T_c superconductivity in $PuCoGa_5$ [5], a modulated superconducting phase in $CeCoIn_5$ that is a strong candidate for the Fulde-Ferrell-Larkin-Ovchinnikov (FFLO) state [6], a possible quadrupolar-related order in $NpFeGa_5$ [7], etc. We ascribe the exotic behavior of these systems to strong electron correlations and spin-orbit coupling; it is deeply related with the magnetism. In this context, it is useful to determine the dynamic magnetic susceptibility of such systems in detail.

$UPtGa_5$ is an itinerant antiferromagnetic (AFM) compound with Néel temperature $T_N = 26$ K [8]. The Sommerfeld coefficient $\gamma = 57$ mJ/mol K^2 indicates that this system is a weak heavy-fermion system. The magnetic structure of the ordered state has been determined with neutron diffraction measurements [9]. The correlation wave vector is $\vec{q}_{\rm cor} = (0,0,\pi/c)$, with the ordered AFM moment along the c axis; thus Ising-type anisotropy is strong in this system. The small 0.24 μ_B AFM ordered moment reflects the itinerant nature of this compound.

Although no superconductivity has been found in $UPtGa_5$, this compound is ideal for understanding the itinerant magnetism of a 115 system via NMR, since the magnetic correlation is simple, i.e., $\vec{q}_{\rm cor}$ is commensurate, with Ising anisotropy, and no T-dependent hyperfine (HF) coupling is observed [10], in contrast with $CeCoIn_5$ [11] and $CeIrIn_5$ [12]. In a previous paper [10], static properties such as bulk magnetic susceptibility and the Knight shift have been reported for $UPtGa_5$. Based on that study, the dynamical magnetic susceptibility is deduced here quantitatively from spin-lattice relaxation data. In comparison with $UPtGa_5$, the sharp contrast with quantum critical metals such as $CeRhIn_5$, $CeCoIn_5$ and $CeIrIn_5$ is revealed. Anomalous HF coupling in the [001], i.e., basal plane, is also clarified. The present study suggests a general method to determine the dynamical susceptibility in magnetic compounds by means of NMR, underlining the importance of complete, detailed experimental results for understanding the electronic state. Since an inelastic neutron scattering measurement is difficult in neutron-absorbent In-based compounds, the determination of dynamical susceptibility by NMR is particularly useful for such a case.

II. EXPERIMENTAL

High-quality single-crystal samples of $UPtGa_5$ were grown by the self-flux method [8]. A characterization of the samples used has been reported previously [8]. NMR signal amplitudes were obtained for ^{69}Ga and ^{195}Pt using fast Fourier transformation (FFT) of spin-echo signals at constant applied magnetic field $H = 7.2416$ T parallel to the a and c axes. The gyromagnetic ratios of ^{69}Ga ($I = 3/2$) and ^{195}Pt ($I = 1/2$) are $\gamma_{\rm Ga}/(2\pi) = 9.093$ MHz/T and $\gamma_{\rm Pt}/(2\pi) = 10.219$ MHz/T, respectively. Spin-lattice relaxation times (T_1) were measured using the inversion and spin-echo recovery method. The relaxation data were a good fit to the expected relaxation functions for $I = 3/2$ and $1/2$ [13].

III. DETAILED ANALYSIS

A. Crystal structure and NMR sites

Figure 1 shows the crystal structure of $UPtGa_5$ ($P4/mmm$). There are two inequivalent Ga sites, the Ga(1) (1c) site and the Ga(2) (4i) site, and one Pt (1b) site. When $H \parallel a$ axis, there are two inequivalent Ga(2) sites: Ga(2a) and Ga(2b). The principal axis of the electric field gradient tensor $\vec{V}_{zz}$ [14] at the Ga(2) site is indicated in Fig. 1. The applied field H is parallel and perpendicular to the principal axis $\vec{V}_{zz}$ for the Ga(2a) and Ga(2b) sites, respectively. Since the spin-lattice relaxation processes are essentially identical for the Ga(2a) and Ga(2b) sites in $UPtGa_5$, results for the Ga(2a) site are mainly presented in this report.

In the formulas below, the subscript α [= Ga(1), Ga(2a,2b) or Pt] indicates parameters for those respective sites. The subscripts $i = a$ and c indicate components along the a and c axes, respectively.

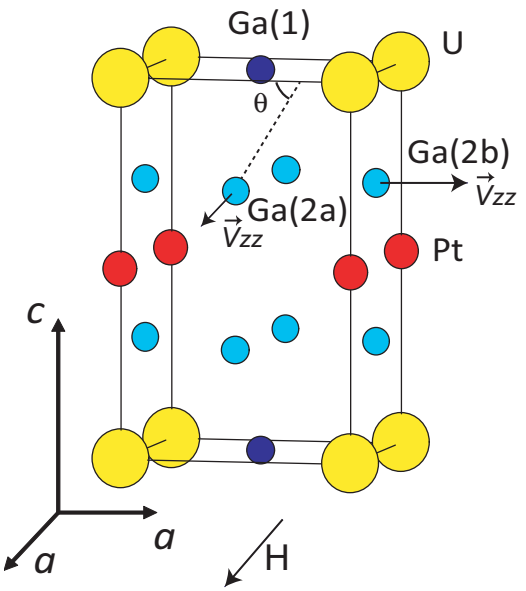

FIG. 1. Crystal structure of $UPtGa_5$. $\vec{V}_{zz}$ indicates the principal axis of the electric field gradient tensor at the Ga(2) site. When the applied field H is parallel to the a axis as indicated in the figure, their low symmetry gives rise to inequivalent Ga(2a) and Ga(2b) sites. The Ga(2) sites are equivalent for the $H \parallel c$ case. The broken line represents the direction of principal axis of HF tensor at Ga(2) site, which has an angle θ with [100] direction.

B. Knight shifts and hyperfine coupling constants

The T dependence of the static magnetic susceptibility χ_i (Fig. 2) and Knight shift $K_{\alpha,i}$, and the $K_{\alpha,i}$ versus χ_i plots have been presented in a previous report [10]. The T dependence of

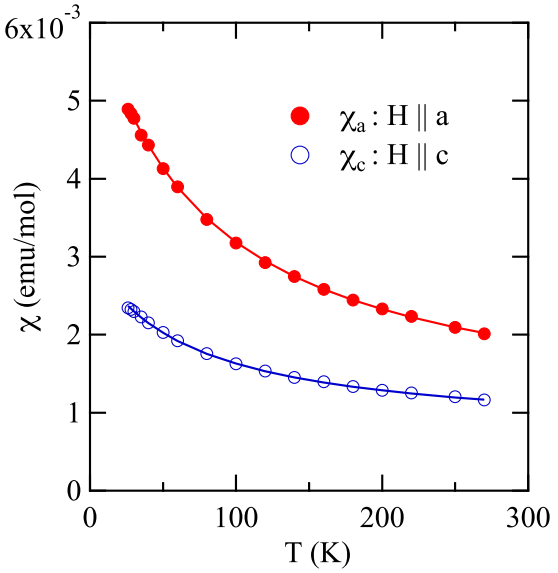

FIG. 2. T dependence of the static magnetic susceptibility χ_i in $UPtGa_5$ [10]. Solid lines are calculated using Eq. (1) with parameters from Table I.

TABLE I. Curie constants, Weiss temperatures, orbital susceptibility terms, and effective moments for the static susceptibilities [10].

	$H \parallel a$ $(i = a)$	$H \parallel c$ $(i = c)$
C_i (emu/mol K)	0.41	0.15
Θ_i (K)	−74	−65
$\chi_{\mathrm{orb},i}$ (10^{-3} emu/mol)	0.83	0.72
$\mu_{\mathrm{eff},i}$ (μ_B)	1.8	1.1

$\chi_{\mathrm{spin},i}$ follows Curie-Weiss behavior in the paramagnetic state:

$$\chi_i = \chi_{\mathrm{spin},i} + \chi_{\mathrm{orb},i}, \quad \chi_{\mathrm{spin},i} \cong \frac{C_i}{T - \Theta_i}, \tag{1}$$

where C_i is the Curie constant, Θ_i is the Weiss temperature, and $\chi_{\mathrm{orb},i}$ is the T-independent, orbital-related susceptibility (Table I). The reduced effective moment $\mu_{\mathrm{eff},i}$ compared to the value of free Ce^{3+} ion indicates the itinerant nature of the system.

The Knight shifts and spin-lattice relaxation at the Ga and Pt ligand sites probe static and dynamic transferred HF fields from the magnetic U site, respectively. A linear relation between Knight shifts $K_{\alpha,i}$ at the Ga(1), Ga(2), and Pt sites and the static susceptibility χ_i has been confirmed in all cases, implying that the transferred HF coupling constants $A_{\alpha,i}$ are T-independent in the paramagnetic state. Thus

$$K_{\alpha,i} = A_{\alpha,i}\chi_{\mathrm{spin},i} + K_{\mathrm{orb},\alpha,i}, \tag{2}$$

where $K_{\mathrm{orb},\alpha,i} = A_{\mathrm{orb},\alpha,i}\chi_{\mathrm{orb},i}$ is the T-independent orbital Knight shift ($A_{\mathrm{orb},\alpha,i}$ is the HF coupling constant for $\chi_{\mathrm{orb},i}$).

C. Spin-lattice relaxation rate $1/T_1$

The spin-lattice relaxation rate $1/T_1$ is a $\vec{q}$ sum over the Brillouin zone (BZ) of the dynamical susceptibility $\mathrm{Im}\chi(\vec{q},\omega)/\omega$ times a $\vec{q}$-dependent HF form factor $F(\vec{q})^2$ with subscripts that denote the ligand site and the fluctuation axis. We present and analyze here a relatively complete set of T_1 data in order to gain a deep insight into the nature of the dynamic susceptibility in $UPtGa_5$. The essential considerations for HF couplings in 115 systems have been presented by Curro [15]. Here we adopt his model. The general expression for T_1T in this kind of system is [13]

$$1/(T_{1,\alpha,j}T) = \gamma_\alpha^2 \sum_i \sum_{\vec{q}} F_{\alpha,i}^2(\vec{q})\mathrm{Im}\,\chi_i(\vec{q},\omega_\alpha)/(\omega_\alpha n_\alpha), \tag{3}$$

where α designates the ligand [Ga(1), Ga(2a), Ga(2b), Pt]; the NMR frequencies $\omega_{\mathrm{Ga}(1,2a,2b)} = \gamma_{\mathrm{Ga}}H$; $\omega_{\mathrm{Pt}} = \gamma_{\mathrm{Pt}}H$; j designates the quantization axis for T_1, i.e., the direction of applied magnetic field H; $\sum_i$ goes over the axes contributing to the relaxation process; and n_α [$n_\alpha = 4$ for Ga(1), $n_\alpha = 2$ for Ga(2) and Pt] is the number of the nearest-neighbor (n.n.) U ions for the α ligand, i.e., the number making identical contributions to the $A_{\alpha,i}$ coefficients given in Table II. Generally, $\sum_i$ covers the two mutually perpendicular directions that are both $\perp$ j axis. The HF form factors $F_{\alpha,j}(\vec{q})$ are defined in detail below.

TABLE II. Transferred hyperfine coupling constants in units of kOe/μ_B at the Ga(1), Ga(2), and Pt sites for $H \parallel a,c$ [10]. As the Ga(2a,2b) sites are equivalent for the $H \parallel c$ case, $A_{\mathrm{Ga(2a)},c} = A_{\mathrm{Ga(2b)},c}$.

	$H \parallel a\ (i=a)$	$H \parallel c\ (i=c)$
$A_{\mathrm{Ga(1)},i}$	9.65	42.0
$A_{\mathrm{Ga(2a)},i}$	19.8	10.2
$A_{\mathrm{Ga(2b)},i}$	16.8	10.2
$A_{\mathrm{Pt},i}$	41.3	87.3

For the purpose of further discussion below (see Sec. III E), we define the magnetic fluctuation strengths $R_{\alpha,i}$ as

$$R_{\alpha,i} \equiv \sum_{\vec{q}} F^2_{\alpha,i}(\vec{q})\mathrm{Im}\chi_i(\vec{q},\omega_\alpha)/\omega_\alpha, \tag{4}$$

where $\mathrm{Im}\chi_i$ is subscripted in case the spin susceptibility, itself, may be anisotropic [13]. Then from Eq. (3) and (4) we may express $1/(T_{1,\alpha,j}T)$ for ligand α with a field along the j axis,

$$\begin{aligned} 1/(T_{1,\alpha,c}T) &= 2\gamma_\alpha^2 R_{\alpha,a}/n_\alpha, \\ 1/(T_{1,\alpha,a}T) &= \gamma_\alpha^2(R_{\alpha,a}+R_{\alpha,c})/n_\alpha. \end{aligned} \tag{5}$$

In Sec. III E, the values of $R_{\alpha,i}$ derived from experiment are combined with values of the $A_{\alpha,i}$ coefficients from Table II to estimate the "characteristic spin fluctuation energy" that underpins the dynamic susceptibility. First, we need to spell out the HF form factors $F_{\alpha,i}(\vec{q})$.

D. Hyperfine form factors $F_{\alpha,i}(\vec{q})$

Owing to the $\vec{q}$ dependence of the HF form factors $F_{\alpha,i}(\vec{q})$, each site probes $\mathrm{Im}\chi_i(\vec{q},\omega_\alpha)/\omega_\alpha$ in different regions of $\vec{q}$ space. In preparation for our interpretation of the entire body of T_1 data on the ligands in $UPtGa_5$, we enumerate here the HF form factors [15] for the Ga(1), Ga(2a,2b) and Pt sites.

For the Ga(1) site, the HF form factors are

$$\begin{aligned} F^2_{\mathrm{Ga(1)},a}(\vec{q}) &= 4A^2_{\mathrm{Ga(1)},a}[\cos^2(q_x a/2)\cos^2(q_y a/2) \\ &\quad +\delta_1^2\sin^2(q_x a/2)\sin^2(q_y a/2)], \\ F^2_{\mathrm{Ga(1)},c}(\vec{q}) &= 4A^2_{\mathrm{Ga(1)},c}\cos^2(q_x a/2)\cos^2(q_y a/2), \end{aligned} \tag{6}$$

where the coefficient δ_1 is nonzero, because the basal plane HF coupling tensor is anisotropic (i.e., different coupling coefficients parallel and perpendicular to the radius vector). This gives rise to an off-diagonal term in the HF coupling tensor for Ga(1) [15]. The resulting δ_1 parameter can be estimated with spin-lattice relaxation data, as will be shown below. From Eqs. (4) and (6), $R_{\mathrm{Ga(1)},i}$ probes the ferromagnetic (FM) correlations in the basal plane, but is insensitive to correlations along the c axis.

At the Ga(2a) site, the HF form factor is

$$\begin{aligned} F^2_{\mathrm{Ga(2a)},a}(\vec{q}) &= 2A^2_{\mathrm{Ga(2b)},a}\left[\cos^2(q_x a/2)+\delta_{2a}^2\sin^2(q_x a/2)\right], \\ F^2_{\mathrm{Ga(2a)},c}(\vec{q}) &= 2A^2_{\mathrm{Ga(2a)},c}\left[\cos^2(q_x a/2)+\delta_{2c}^2\sin^2(q_x a/2)\right], \end{aligned} \tag{7}$$

where, again, the off-diagonal terms involving $2\delta_{2a}$ and δ_{2c} are estimated from spin-lattice relaxation data (see below). As with the Ga(1) site, $R_{\mathrm{Ga(2)},i}$ probes FM correlations in the basal plane, but is rather insensitive to correlations along the c axis from Eqs. (4) and (7).

At the Pt site, the HF form factor is

$$\begin{aligned} F^2_{\mathrm{Pt},a}(\vec{q}) &= 2A^2_{\mathrm{Pt},a}\cos^2(q_z c/2), \\ F^2_{\mathrm{Pt},c}(\vec{q}) &= 2A^2_{\mathrm{Pt},c}\cos^2(q_z c/2), \end{aligned} \tag{8}$$

indicating that AFM correlations along the c axis are filtered out for $R_{\mathrm{Pt},i}$, in addition to being insensitive to the correlations in the basal plane.

Regarding the correlation vector $\vec{q}_{\mathrm{cor}} = (0,0,\pi/c)$ for $UPtGa_5$, the Ga(1) and Ga(2) sites do probe the FM correlations of the basal plane, but are rather insensitive to the AFM correlations along the c axis. The Pt site does not probe correlations near $\vec{q}_{\mathrm{cor}} = (0,0,\pi/c)$, either.

Generally, if there is no correlation between the fluctuations at magnetic sites, i.e., $\mathrm{Im}\chi(\vec{q},\omega_\alpha)$ is independent of $\vec{q}$, then there are n_α independent contributions of $2\gamma_\alpha^2(A_\alpha/n_\alpha)^2\mathrm{Im}\chi(\vec{q},\omega_\alpha)/\omega_\alpha$ from magnetic sites to $1/(T_1T)$ at an α ligand site. Thus the relation $1/(T_1T) = 2\gamma_\alpha^2(A_\alpha^2/n_\alpha)\mathrm{Im}\chi(\vec{q},\omega_\alpha)/\omega_\alpha$ should be satisfied at the ligand site, which corresponds to the relation $R_{\alpha,i} = A^2_{\alpha,i}\mathrm{Im}\chi_i(\vec{q},\omega_\alpha)/\omega_\alpha$ for the present case. It follows that $\Sigma_{\vec{q}}F^2_{\alpha,i}(\vec{q})/A^2_{\alpha,i} = 1$ [note that $A_{\mathrm{Ga(2b)},a}$ should be adopted here for $R_{\mathrm{Ga(2a)},a}$ and $F^2_{\mathrm{Ga(2a)},a}$ from Eq. (7)]. In fact, this relation is satisfied for the Pt site, i.e., for Eq. (8). On the other hand, this relation is not satisfied for $F^2_{\mathrm{Ga(1)},a}(\vec{q})$ and $F^2_{\mathrm{Ga(2a)},i}(\vec{q})$ at the Ga(1) and Ga(2) sites, owing to the finite values for δ_1 and $\delta_{2a,2c}$. Thus we have

$$\begin{aligned} \Sigma_{\vec{q}}F^2_{\mathrm{Ga(1)},a}(\vec{q})/A^2_{\mathrm{Ga(1)},a} &= 1+\delta_1^2, \\ \Sigma_{\vec{q}}F^2_{\mathrm{Ga(2a)},a}(\vec{q})/A^2_{\mathrm{Ga(2b)},a} &= 1+\delta_{2a}^2, \\ \Sigma_{\vec{q}}F^2_{\mathrm{Ga(2a)},c}(\vec{q})/A^2_{\mathrm{Ga(2a)},c} &= 1+\delta_{2c}^2. \end{aligned} \tag{9}$$

These equations indicate that the HF coupling constant should be replaced by an effective value for $A_{\alpha,\mathrm{eff},i}$, in order to preserve the normalization relation $\Sigma_{\vec{q}}F^2_{\alpha,i}(\vec{q})/A^2_{\alpha,\mathrm{eff},i} = 1$. Henceforth, we take

$$\begin{aligned} A_{\mathrm{Ga(1)},\mathrm{eff},a} &\equiv \left(1+\delta_1^2\right)^{0.5}A_{\mathrm{Ga(1)},a}, \\ A_{\mathrm{Ga(2a)},\mathrm{eff},a} &\equiv \left(1+\delta_{2a}^2\right)^{0.5}A_{\mathrm{Ga(2b)},a}, \\ A_{\mathrm{Ga(2a)},\mathrm{eff},c} &\equiv \left(1+\delta_{2c}^2\right)^{0.5}A_{\mathrm{Ga(2a)},c}. \end{aligned} \tag{10}$$

E. Characteristic spin fluctuation energy Γ_i

At low levels of spin correlation, the dynamical susceptibility can be approximated using the $\vec{q}$-averaged characteristic spin fluctuation energy Γ_i [16] giving

$$\mathrm{Im}\chi_i(\vec{q},\omega_\alpha)/\omega_\alpha \simeq \chi_{\mathrm{spin},i}/\Gamma_i. \tag{11}$$

We substitute the foregoing expression into Eq. (4) and combine the result with Eqs. (9) and (10) to define the quantity

$$\begin{aligned} \Phi_{\alpha,i} &\equiv \frac{R_{\alpha,i}}{A^2_{\alpha,\mathrm{eff},i}\chi_{\mathrm{spin},i}} = \frac{1}{\Gamma_i}\Sigma_{\vec{q}}F^2_{\alpha,i}(\vec{q})/A^2_{\alpha,\mathrm{eff},i} \\ &\simeq \frac{1}{\Gamma_i} \text{ for the uncorrelated case.} \end{aligned} \tag{12}$$

If correlations are negligible, then the $\Phi_{\alpha,i}$ evaluated using experimental data for $T_{1,\alpha,i}$ and for $\chi_{\mathrm{spin},i}$ can be used to estimate Γ_i. Note that for each axis, in the low correlation limit, Γ_i is expected to be independent of ligand site. In order for the site independence of Γ_i to be realized, reasonably accurate values of δ_1, δ_{2a}, and δ_{2c} must be used in Eq. (10). In the next section, we describe how suitable values for the δ's have been chosen.

IV. EXPERIMENTAL RESULTS

In Fig. 3, a comprehensive body of T_1 data for all three ligand sites in $UPtGa_5$ taken with a single-crystal specimen is plotted in a log-log format as $1/T_1T$ versus T. The plot is limited to the paramagnetic region, extending from $T = 26$ up to 260 K. For Ga(1) and Pt, there are two plots each for the two distinguishable axes; for Ga(2) there are data for all three distinguishable axes. However, for Ga(2b), the limited number of points shown are seen to coincide with the Ga(2a) plot for the field oriented in the basal plane. Only the Ga(2a) case will be discussed below.

A. T dependence of $1/(T_{1,\alpha,i}T)$

At higher temperatures, all six of the data plots in Fig. 3 vary in a fashion roughly consistent with $T_1 \sim$ constant, indicating that the localized character remains in effect up to high temperatures. As T is lowered, the Ga site data plots all exhibit an increase in $1/T_1T$ that we ascribe to the onset of critical fluctuations on approaching the AFM transition. The basal-plane fluctuations are clearly contributing to this upturn for Ga(1) ($H \parallel c$) and Ga(2a)($H \parallel c$), since c axis fluctuations are not involved for those cases. However, c axis fluctuations are also very strong, as evidenced by the marked upturns in the data curves for Ga(1) and Ga(2) for ($H \parallel a$). Remarkably, the Pt sites are not sensitive to the AFM critical fluctuations. They are subject to both in-plane and c axis transferred HF fluctuations, but in both cases the form factor [Eq. (8)] imposes a broad minimum with a zero at $\vec{q} = \vec{q}_{\mathrm{cor}}$. See the next section for more discussion of the Pt results. On the other hand, the increase in critical-fluctuation behavior near the AFM transition for the Ga(1) and Ga(2) shows that these fluctuations extend into the q_x and q_y axes near T_N, since the $F_{\mathrm{Ga(1,2a,2b)},i}$ have no component involving q_z, but have peaks near the center of the BZ involving $\delta_{1,2a,2c}$ [see Eqs. (6) and (7)].

B. Comparison of $\Phi_{\alpha,i}$ at different sites

In Fig. 4, we display the T dependence of six independent curves for $\Phi_{\alpha,i}$, calculated with Eqs. (4) and (12) using the approximation given in Eq. (11) and the T_1 data shown in Fig. 3. In constructing the data plotted in Fig. 4, there are two objectives in mind. The first is to determine the value of Γ_i associated with each Φ plot, and the second is to determine the values of $\delta_{1,2a,2c}$ parameters that will give consistent values for Γ_i that characterize each type of fluctuations (i.e., c axis and basal plane).

First, we can construct curves for $\Phi_{\mathrm{Ga(1)},c}$ and $\Phi_{\mathrm{Ga(2)},c}$, using Eq. (4) with $\chi_{\mathrm{spin},c}$. $\Phi_{\mathrm{Ga(1)},c}$ has no adjustable parameters, and thus by itself determines an experimental value for $\Gamma_c \sim 8$ meV. The curve for $\Phi_{\mathrm{Ga(2)},c}$ then is adjusted to coincide with the high-T (minimum correlation) end of that for $\Phi_{\mathrm{Ga(1)},c}$ by selecting $|\delta_{2c}| = 0.95$, giving the excellent correspondence shown in Fig. 4. This rather small correlation energy for the c axis is roughly consistent with the AFM ordering at $T_N = 28$ K. However, it is a bit peculiar that the c-axis curve $\Phi_{\mathrm{Pt},c}$ that has no adjustable parameter, deviates widely from the other two. The ostensible justification for this behavior is that the form factor $\sim \cos^2(q_z c/2)$ cuts a large hole in the BZ just where the dominant c-axis AFM fluctuations reside. As a result, $\Phi_{\mathrm{Pt},c}$ ends up being dominated by much "harder" fluctuations around the edges of the BZ. See below for further discussion of the inconsistency among the $\Phi_{\alpha,c}$.

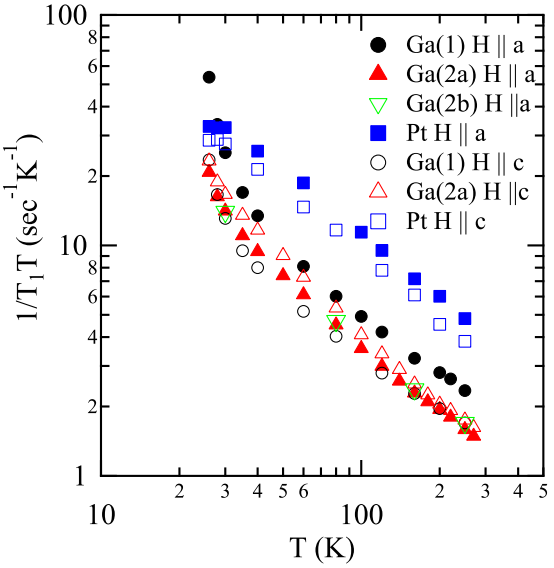

FIG. 3. T dependence of $1/(T_1T)$ at Ga(1), Ga(2) and Pt sites for $H \parallel a,c$ axes in the paramagnetic state of $UPtGa_5$. Size of symbols corresponds to the experimental errors.

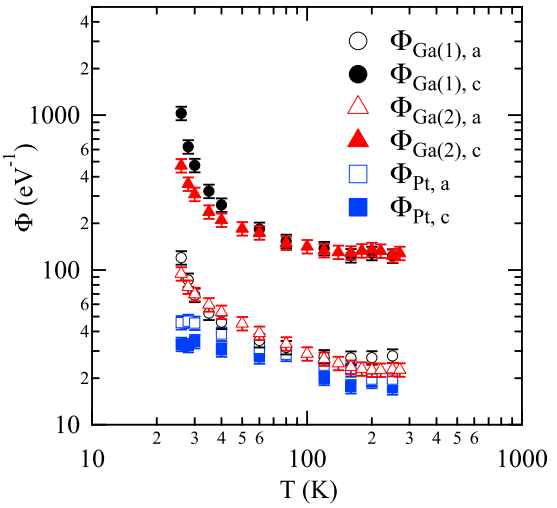

FIG. 4. T dependence of $\Phi_{\alpha,i}$. At high temperatures, $\Phi_{\alpha,i}$ is independent of α except $\Phi_{\mathrm{Pt},c}$, whereupon it then corresponds to $1/\Gamma_i$.

Concerning the fluctuations in the basal plane, the asymptotic high-temperature value of $\Phi_{\mathrm{Pt},a}$ sets the scale for Γ_a, since there are no adjustable parameters for $\Phi_{\mathrm{Pt},i}$. Next, curves for $\Phi_{\mathrm{Ga}(1),a}$ and $\Phi_{\mathrm{Ga}(2),a}$ are brought into approximate coincidence with $\Phi_{\mathrm{Pt},a}$ with the estimates $|\delta_1| = 4.3$ and $|\delta_{2a}| = 0.9$. The results are plotted in the lower cluster of curves in Fig. 4. At the high-temperature (260 K) end of these curves, basal-plane fluctuations would be least correlated, giving a site-independent estimate $\Gamma_a \sim 43$ meV. These values are reasonable, giving a nicely consistent picture for the basal-plane fluctuations.

It is remarkable that no large difference is found between $\Phi_{\mathrm{Pt},a}$ and $\Phi_{\mathrm{Pt},c}$ at the Pt site, in spite of dramatically different values for Γ_a and Γ_c. Since the fluctuations with $\vec{q} \sim \vec{q}_{\mathrm{cor}}$ cancel at the Pt site, this means that the Ising anisotropy appears only in the vicinity of $\vec{q}_{\mathrm{cor}}$. This is a characteristic of itinerant magnetism in which correlations localize around a certain $\vec{q}$ vector.

At all temperatures, $\Phi_{\mathrm{Ga}(1,2),c}$ is larger than $\Phi_{\mathrm{Ga}(1,2),a}$, indicating that Γ_c is expected to be smaller than Γ_a. Thus $\mathrm{Im}\chi_c > \mathrm{Im}\chi_a$, which is consistent with having the AFM ordered moment along the c axis. In contrast, the static magnetic susceptibility at $q = 0$ has the opposite anisotropy, i.e., $\chi_{\mathrm{spin},a} > \chi_{\mathrm{spin},c}$ (Fig. 2). This difference indicates again that the Ising anisotropy appears only in the vicinity of $\vec{q}_{\mathrm{cor}}$. Actually, similar opposite anisotropy between Γ and χ is confirmed in $CeCoIn_5$ [17] and $CeIrIn_5$ [12].

V. DISCUSSION

A. Hyperfine coupling anomaly

Using the estimated $|\delta_{2a,2c}|$ at the Ga(2a) site, the HF field at the Ga(2) site can be decomposed based on the previous simplified model [15]:

$$\begin{aligned} &B_0 \equiv (B_\parallel + B_\perp)/2, \quad B_A \equiv (B_\parallel - B_\perp)/2, \\ &A_{\mathrm{Ga}(2\mathrm{b}),a} \simeq 2(B_0 + B_A\cos\theta), \quad \delta_{2a}A_{\mathrm{Ga}(2\mathrm{b}),a} \simeq 2B_A\sin\theta, \\ &A_{\mathrm{Ga}(2\mathrm{a}),c} \simeq 2(B_0 - B_A\cos\theta), \quad \delta_{2c}A_{\mathrm{Ga}(2\mathrm{a}),c} \simeq 2B_A\sin\theta, \end{aligned} \tag{13}$$

where $B_\parallel$ and $B_\perp$ are the HF coupling constants parallel and perpendicular to the principal axis of Ga(2) HF tensor; θ is the angle between the [100] direction and the principal axis of HF tensor, which may be in the (010) plane (see Fig. 1). These relations can be satisfied roughly with $B_\parallel \sim 13$ kOe/μ_B, $B_\perp \sim 0.2$ kOe/μ_B, and $\theta \sim 75$ degree if positive $\delta_{2a,2c}$ are adopted. Although θ is expected to be ~ 45 degrees in a simple model [15], the deviation from that value might be acceptable considering the simplified nature of the model. If negative $\delta_{2a,2c}$ are adopted, a reasonable θ value can not be obtained.

Concerning T_1 at the Ga(2b) site, another HF coupling constant B_y may be introduced [15]. B_y is parallel to $\vec{v}_{zz}$, but perpendicular to H [15]. Since the T_1 is almost the same at the Ga(2a) and Ga(2b) sites, the following relation is suggested:

$$\left(1 + \delta_{2a}^2\right)^{0.5} A_{\mathrm{Ga}(2\mathrm{b}),a} \simeq 2B_y. \tag{14}$$

Although its generality is not evident, the HF coupling at the Ga(2) site is nearly isotropic in the plane perpendicular to the c axis of $UPtGa_5$, supported by the fact that $A_{\mathrm{Ga}(2\mathrm{a}),a}$ is quite similar to $A_{\mathrm{Ga}(2\mathrm{b}),a}$ (Table, II). As $\mathrm{Im}\chi_c > \mathrm{Im}\chi_a$, the spin-lattice relaxation at the Ga(2) site is dominated by fluctuations along the c axis. Thus the small difference between $A_{\mathrm{Ga}(2\mathrm{a}),a}$ and $A_{\mathrm{Ga}(2\mathrm{b}),a}$ may be quite difficult to resolve in T_1 measurements.

On the other hand, the large value of $|\delta_1| \sim 4.3$ obtained for the Ga(1) site was unexpected, but could be rationalized with the scenario we now describe. For the case of Ga(1), one has

$$\begin{aligned} &B_0 \equiv (B_\parallel + B_\perp)/2, \quad B_A \equiv (B_\parallel - B_\perp)/2, \\ &A_{\mathrm{Ga}(1),a} \simeq 4B_0, \quad \delta_1 A_{\mathrm{Ga}(1),a} \simeq 4B_A, \end{aligned} \tag{15}$$

where $B_\parallel$ and $B_\perp$ are the HF coupling constants parallel and perpendicular to the U-Ga(1) radius vector, respectively. It is important to note that the adjustment of δ_1 to obtain a suitable curve for $\Phi_{\mathrm{Ga}(1),a}$ only determines the magnitude of δ_1, so that when we combine the last two of the Eq. (15), what we actually find is $B_A = \pm\delta_1 B_0$. Using the first two equations, we then find $B_\parallel = B_\perp(1+\delta_1)/(1-\delta_1)$ if δ_1 is positive and the same with $B_\parallel$ and $B_\perp$ reversed if it is negative. Using $A_{\mathrm{Ga}(1),a} = 9.65$ kOe/μ_B from Table II, one then finds that $(B_\parallel, B_\perp) = (-8.0, 12.8)$ kOe/μ_B, except that we do not know which is which. A possible resolution of this puzzle might be effected by invoking $B_c \equiv A_{\mathrm{Ga}(1),c}/4 = 10.5$ kOe/μ_B (Table II). In terms of the RKKY plus pseudodipolar mechanism for transferred HF couplings, one might suppose that $B_\perp$ and B_c are closely related, both being perpendicular to the radius vector, differing only in that one is in the basal plane, the other perpendicular to it. This comparison would strongly suggest that $B_\perp = 12.8$ and $B_\parallel = -8.0$ kOe/μ_B with the negative $\delta_1 = -4.3$. Viewed in this light, the seemingly large value for $|\delta_1|$ appears more reasonable.

In $UPtGa_5$, the values of $\delta_{1,2a,2c}$ are all found to be appreciable; among 115 compounds these parameters would be expected to vary widely. Beyond $UPtGa_5$, the value of δ_1 must certainly be substantial in order to explain the internal field at the In(1) site in the antiferromagnetically ordered state of $CeRhIn_5$ [15]. In contrast, the values $\delta_{1,2a,2c} \sim 0$ are likely in the In(1,2) sites of $CeCoIn_5$ [17] and $CeIrIn_5$ [12]. Although the microscopic origin of these differences is still unclear, the present study shows that complete HF coupling tensor data can lead to an accurate characterization of the dynamic susceptibility. The importance of comprehensive NMR measurements should be emphasized.

B. $\vec{q}$ dependence of dynamical susceptibility and correlation length

In order to treat the $\vec{q}$ dependence of $\mathrm{Im}\chi(\vec{q},\omega_n)$ at $\vec{q} = \vec{q}_{\mathrm{cor}} + \delta\vec{q}$, the following equation under the condition $\Gamma(\vec{q}) \gg \omega_\alpha$ is adopted [16] for $\delta\vec{q} \sim \vec{q}_B$ ($\vec{q}_B$ is the BZ boundary vector):

$$\begin{aligned} \frac{\mathrm{Im}\chi(\vec{q},\omega_\alpha)}{\omega_\alpha} &\simeq \frac{\chi(\vec{q})\Gamma(\vec{q})}{\Gamma(\vec{q})^2 + \omega_\alpha^2} \simeq \frac{\chi_L\Gamma_L}{\Gamma(\vec{q})^2} \\ &\simeq \frac{\chi_L\Gamma_L}{\Gamma(\vec{q}_{\mathrm{cor}})^2[1 + 0.5(\vec{\xi}\delta\vec{q}/\pi)^2]^2}, \end{aligned} \tag{16}$$

where $\vec{\xi}$ is the magnetic correlation length, and χ_L and Γ_L are the local susceptibility and spin fluctuation energy, respectively. A correction factor 0.5 is adopted to treat $\delta\vec{q} \sim$

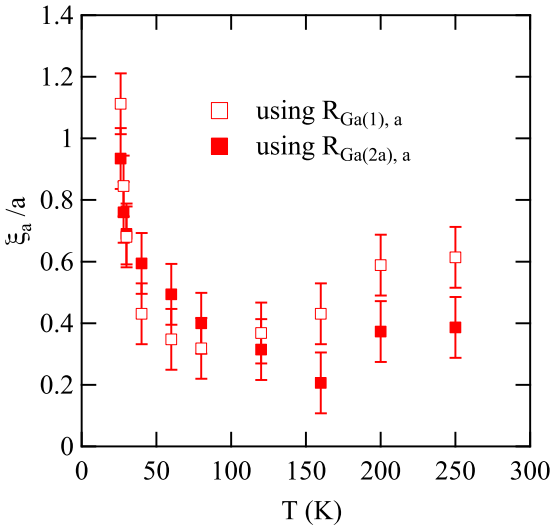

FIG. 5. T dependence of ξ_a/a in the basal plane. Based on Eq. (17), ξ_a/a is estimated using $R_{\mathrm{Ga}(1),a}$ and $R_{\mathrm{Ga}(2a),a}$.

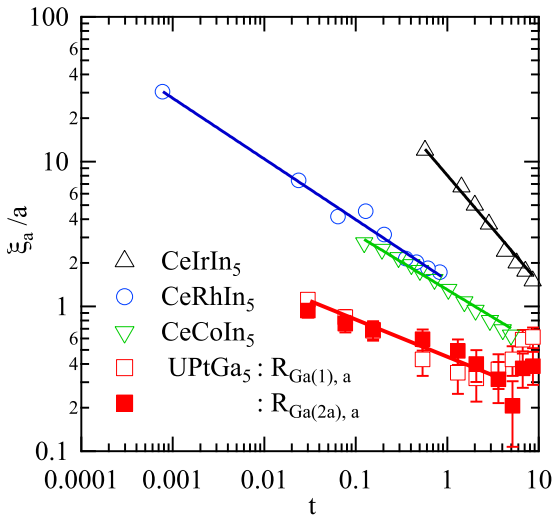

FIG. 6. T dependence of correlation length ξ_a/a in the basal plane of $CeIrIn_5$ [12], $CeCoIn_5$ [3], and $CeRhIn_5$ [18] compared with the present ξ_a/a of $UPtGa_5$ shown in Fig. 5. Here, $t \equiv 2T/\Gamma_a$ for paramagnets $CeIrIn_5$ ($\Gamma_a \sim 7$ K) and $CeCoIn_5$ ($\Gamma_a \sim 4$ K), $t \equiv (T - T_N)/T_N$ for antiferromagnets $CeRhIn_5$ ($T_N = 3.8$ K) and $UPtGa_5$ ($T_N = 26$ K). Solid lines represent $\xi_a/a \sim t^{-\nu}$; $\nu \sim 0.75$ for $CeIrIn_5$, $\nu \sim 0.4$ for $CeRhIn_5$, and $CeCoIn_5$ and $\nu \sim 0.25$ for $UPtGa_5$. The correlation in the basal plane is more enhanced in superconducting $CeIrIn_5$, $CeCoIn_5$, and $CeRhIn_5$, since these compounds are considered to be near the quantum critical point.

$\vec{q}_B$. Considering the FM correlations in the basal plane along the a axis and the HF form factors which are insensitive to the AFM correlation along the c axis in $UPtGa_5$, one finds the following approximate relations:

$$\frac{R_{\mathrm{Pt},a}}{A^2_{\mathrm{Pt},a}} \sim \frac{\chi_L \Gamma_L}{\Gamma(\vec{q}_{\mathrm{cor}})^2\{1 + 0.5(\xi_a/a)^2\}^2},$$
$$\times \frac{R_{\mathrm{Ga}(1,2a),a}}{A^2_{\mathrm{Ga}(1,2a),\mathrm{eff},a}} \sim \frac{\chi_L \Gamma_L}{\Gamma(\vec{q}_{\mathrm{cor}})^2},$$
$$\times \frac{R_{\mathrm{Ga}(1,2a),a} A^2_{\mathrm{Pt},a}}{R_{\mathrm{Pt},a} A^2_{\mathrm{Ga}(1,2a),\mathrm{eff},a}} \sim [1 + 0.5(\xi_a/a)^2]^2,$$
$$\xi_a/a \sim \sqrt{2}\left[\left(\frac{R_{\mathrm{Ga}(1,2a),a} A^2_{\mathrm{Pt},a}}{R_{\mathrm{Pt},a} A^2_{\mathrm{Ga}(1,2a),\mathrm{eff},a}}\right)^{0.5} - 1\right]^{0.5}, \quad (17)$$

where the BZ boundary vector in the basal plane $\vec{q}_B = (\pi/a,0,0)$ is adopted for $\delta\vec{q}$ at the Pt site, and ξ_a is the correlation length along the a axis. Figure 5 shows the T dependence of ξ_a. It is shown that there is almost no correlation down to 100 K, then ξ_a increases rapidly below 50 K toward $T_N = 26$ K. Compared with the case of $UPtGa_5$, ξ_a is enhanced in $CeIrIn_5$ [12], $CeCoIn_5$ [3], and $CeRhIn_5$ [18]. Figure 6 shows t dependencies of ξ_a/a in paramagnets $CeIrIn_5$ [12] and $CeCoIn_5$ [3], and antiferromagnets $CeRhIn_5$ [18] for comparison with the present case of $UPtGa_5$. In the spin-fluctuation model [19], a relation $T_N \sim 0.5\Gamma$ can be obtained for typical AFM case. Based on this relation, the normalized temperature t is defined as; $t \equiv 2T/\Gamma_a$ for paramagnet $CeIrIn_5$ ($\Gamma_a \sim 7$ K [12]) and $CeCoIn_5$ ($\Gamma_a \sim 4$ K [3]); in contrast, $t \equiv (T - T_N)/T_N$ for antiferromagnets $CeRhIn_5$ ($T_N = 3.8$ K [18]) and $UPtGa_5$. Not only the absolute ξ_a/a value but also its critical exponent ν of $\xi_a/a \sim t^{-\nu}$ are enhanced in $CeIrIn_5$, $CeCoIn_5$, and $CeRhIn_5$. Around the quantum critical point, quantum critical fluctuations are expected to survive up to high temperatures [20]. Therefore the observed behavior may indicate that these Ce-based compounds are very near to an itinerant quantum critical point. In contrast, the variation of ν remains for future study.

VI. SUMMARY

Through analysis of NMR spin-lattice relaxation tim measurements, the nature of the dynamic magnetic susceptibility in $UPtGa_5$ has been investigated. First, Ising anisotropy appears only in the vicinity the correlation vector $\vec{q}_{\mathrm{cor}} = (0,0,\pi/c)$. While the anisotropy of the characteristic spin fluctuation energy at $\vec{q}_{\mathrm{cor}}$: $\Gamma_a > \Gamma_c$ coincides with the direction of ordered moment along the c axis, it is in fact opposite to the anisotropy of the static susceptibility at $\vec{q} = 0$: $\chi_a > \chi_c$. This suggests a $\vec{q}$ dependence for the spin-fluctuation energy.

In nonsuperconducting $UPtGa_5$, the correlation length decreases rapidly at temperatures above T_N. The latter behavior stands in contrast with unconventional superconductors near quantum critical points such as $CeRhIn_5$ and $CeIrIn_5$, in which the correlations survive up to high temperatures. Empirically, in addition, the AFM-XY anisotropy is favorable for d-wave superconductivity in f-electron systems, as compared with Ising anisotropy [21,22]. For example, $CeCoIn_5$ and $CeIrIn_5$ show the AFM-XY anisotropy [21]. The relationship between the character of the magnetic fluctuations and unconventional superconductivity bears further investigation.

ACKNOWLEDGMENTS

The high quality sample for measurements was prepared by Y. Tokiwa, S. Ikeda, and Y. Onuki, which is greatly appreciated. We are grateful for stimulating discussions with

H. Kato. This work was supported by Japan Society for the Promotion of Science KAKENHI Grants No. 15K05152 and No. 15K05884 (J-Physics), and the REIMEI Research Program of Japan Atomic Energy Agency.

[1] J. L. Sarrao and J. D. Thompson, J. Phys. Soc. Jpn. **76**, 051013 (2007).
[2] T. Park, F. Ronning, H. Q. Yuan, M. B. Salamon, R. Movshovich, J. L. Sarrao, and J. D. Thompson, Nature (London) **440**, 65 (2006).
[3] H. Sakai, S. E. Brown, S.-H. Baek, F. Ronning, E. D. Bauer, and J. D. Thompson, Phys. Rev. Lett. **107**, 137001 (2011).
[4] V. A. Sidorov, M. Nicklas, P. G. Pagliuso, J. L. Sarrao, Y. Bang, A. V. Balatsky, and J. D. Thompson, Phys. Rev. Lett. **89**, 157004 (2002).
[5] J. L. Sarrao, L. A. Morales, J. D. Thompson, B. L. Scott, G. R. Stewart, F. Wastin, J. Rebizant, P. Boulet, E. Colineau, and G. H. Lander, Nature (London) **420**, 297 (2002).
[6] A. Bianchi, R. Movshovich, C. Capan, P. G. Pagliuso, and J. L. Sarrao, Phys. Rev. Lett. **91**, 187004 (2003).
[7] S. Kambe, H. Sakai, Y. Tokunaga, R. E. Walstedt, D. Aoki, Y. Homma, and Y. Shiokawa, Phys. Rev. B **76**, 144433 (2007).
[8] Y. Tokiwa, S. Ikeda, Y. Haga, T. Okubo, T. Iizuka, K. Sugiyama, A. Nakamura, and Y. Onuki, J. Phys. Soc. Jpn. **71**, 845 (2002).
[9] Y. Tokiwa, Y. Haga, N. Metoki, Y. Ishii, and Y. Onuki, J. Phys. Soc. Jpn. **71**, 725 (2002).
[10] H. Kato, H. Sakai, Y. Tokunaga, Y. Tokiwa, S. Ikeda, Y. Onuki, S. Kambe, and R. E. Walstedt, J. Phys. Soc. Jpn. **72**, 2357 (2003).
[11] N. J. Curro, B. Simovic, P. C. Hammel, P. G. Pagliuso, J. L. Sarrao, J. D. Thompson, and G. B. Martins, Phys. Rev. B **64**, 180514(R) (2001).
[12] S. Kambe, H. Sakai, Y. Tokunaga, and R. E. Walstedt, Phys. Rev. B. **82**, 144503 (2010).
[13] R. E. Walstedt, *The NMR probe of High* T_c *Materials* (Springer, Berlin, Heidelberg, 2008).
[14] A. Abragam, *Principles of Nuclear Magnetism* (Clarendon, Oxford, 1961).
[15] N. J. Curro, New J. Phys. **8**, 173 (2006).
[16] Y. Kuramoto and Y. Kitaoka, *Dynamics of Heavy Electrons* (Clarendon, Oxford, 2000).
[17] H. Sakai, S.-H. Baek, S. E. Brown, F. Ronning, E. D. Bauer, and J. D. Thompson, Phys. Rev. B **82**, 020501(R) (2010).
[18] N. J. Curro, J. L. Sarrao, J. D. Thompson, P. G. Pagliuso, S. Kos, Ar. Abanov, and D. Pines, Phys. Rev. Lett. **90**, 227202 (2003).
[19] T. Moriya and T. Takimoto, J. Phys. Soc. Jpn. **64**, 960 (1995).
[20] S. Sachdev, *Quantum Phase Transition* (Cambridge University Press, New York, 2011).
[21] S. Kambe, H. Sakai, Y. Tokunaga, and K. Kaneko, J. Phys. Conf. Series **344**, 012003 (2012).
[22] H. Sakai, S. Kambe, Y. Tokunaga, Y. Haga, S-H. Baek, F. Ronning, E. D. Bauer, and J. D. Thompson, *MRS Symposia Proceedings* No. 1264 (MRS, San Francisco, 2010), p. 69.